# Glut9 is a major regulator of urate homeostasis and its genetic inactivation induces hyperuricosuria and urate nephropathy

Frédéric Preitner[a,b,1], Olivier Bonny[c,1], Alexandra Laverrière[b,d], Samuel Rotman[e], Dmitri Firsov[c], Anabela Da Costa[a,c], Salima Metref[a,c], and Bernard Thorens[b,d,2]

[a]Mouse Metabolic Facility of the Cardiomet Center and [e]Institute of Pathology, University Hospital, 1011 Lausanne, Switzerland; and [b]Center for Integrative Genomics, [c]Department of Pharmacology and Toxicology, and [d]Department of Physiology, University of Lausanne, CH-1015 Lausanne, Switzerland

Edited by Gerhard Giebisch, Yale University School of Medicine, New Haven, CT, and approved July 21, 2009 (received for review April 22, 2009)

**Elevated plasma urate levels are associated with metabolic, cardiovascular, and renal diseases. Urate may also form crystals, which can be deposited in joints causing gout and in kidney tubules inducing nephrolithiasis. In mice, plasma urate levels are controlled by hepatic breakdown, as well as, by incompletely understood renal processes of reabsorption and secretion. Here, we investigated the role of the recently identified urate transporter, Glut9, in the physiological control of urate homeostasis using mice with systemic or liver-specific inactivation of the *Glut9* gene. We show that Glut9 is expressed in the basolateral membrane of hepatocytes and in both apical and basolateral membranes of the distal nephron. Mice with systemic knockout of *Glut9* display moderate hyperuricemia, massive hyperuricosuria, and an early-onset nephropathy, characterized by obstructive lithiasis, tubulointerstitial inflammation, and progressive inflammatory fibrosis of the cortex, as well as, mild renal insufficiency. In contrast, liver-specific inactivation of the *Glut9* gene in adult mice leads to severe hyperuricemia and hyperuricosuria, in the absence of urate nephropathy or any structural abnormality of the kidney. Together, our data show that Glut9 plays a major role in urate homeostasis by its dual role in urate handling in the kidney and uptake in the liver.**

gout | knockout | nephrolithiasis | uric acid

Urate is the end product of purine degradation in humans, whereas in rodents urate is further converted to allantoin by the hepatic enzyme uricase. In human and some apes, the uricase gene has acquired inactivating mutations, which leads to relatively high plasma urate levels: 240–360 $\mu$M in humans vs. 30–50 $\mu$M in mice. Because urate has anti-oxidant properties, high circulating concentrations protect against oxidative stress. However, plasma urate concentrations above the normal range may also be deleterious, and are often associated with the metabolic syndrome and increased risk of hypertension, renal, and cardiovascular diseases (1–3). Elevated urate concentrations also favor formation of urate crystals in the joints, causing gout, and in the kidney, predisposing to urate nephrolithiasis (4, 5). Chronic hyperuricemia and hyperuricosuria in gout patients are frequently associated with a form of nephropathy characterized by tubulointerstitial fibrosis and glomerulosclerosis (6). Acute urate nephropathy can arise as a consequence of chemotherapy-induced tumor lysis, which leads to a surge in urate formation (7).

The kidney plays a crucial role in maintaining plasma urate levels through complex transepithelial transport systems that promote both reabsorption and secretion of urate and that are located largely in the proximal convoluted tubule in humans (8). The urate/anion exchanger URAT1 plays an important role in urate reabsorption across the apical membrane of proximal tubular epithelial cells. Mutations in URAT1 cause hypouricemia in humans (9), further *Urat1* gene knockout in the mouse leads to mild hypouricemia and increased urate excretion (10). The apical membrane organic anion transporter OAT4 may also transport urate (11). On the basolateral side of proximal tubular epithelial cells the exit of urate depends on a voltage-dependent transport system, which may be GLUT9 in humans (12) (see below). The basolateral membrane organic anion transporters OAT1 and OAT3 also transport urate (13, 14). However, inactivation of either OAT1 or OAT3 slightly decreases uricosuria, suggesting that their principal function may be in urate excretion (10).

Recent genetic studies revealed a strong link between urate plasma levels and single nucleotide polymorphisms in the *SLC2A9* gene encoding Glut9, a member of the glucose transporter family highly expressed in liver and kidney (15, 16–18). At least two splice variants have been identified differing only in the length of their amino-terminal cytoplasmic domains. The long form is targeted to the basolateral membrane and the short form to the apical membrane of polarized epithelial cells (19, 20). In the human kidney, Glut9 is present in proximal convoluted tubules, whereas in rodents it is most probably in distal connecting tubules (20). Functional studies confirmed that Glut9 is a urate transporter (18, 21) and mutations in its sequence cause hypouricemia in human subjects (22).

Here, we generated mice with systemic or liver-specific inactivation of the Glut9 gene and describe a major role of Glut9 in urate homeostasis.

## Results

**Generation of Glut9 Knockout Mice.** Mice with a floxed *Glut9* allele were generated using the targeting strategy detailed in Fig. S1*a*. WT and recombined alleles were identified by PCR analysis (Fig. S1*b*), and Western blot analysis of liver membranes showed that expression of Glut9 was reduced by half in $Glut9^{+/-}$ mice and was absent in knockout mice (Fig. S1*c*). Breeding $Glut9^{+/-}$ mice together yielded $Glut9^{-/-}$ (G9KO) mice with approximately half of the expected Mendelian frequency: out of 347 mice, we obtained 35 G9KO, 201 $Glut9^{+/-}$, and 111 $Glut9^{+/+}$ mice, indicating some embryonic lethality in the absence of this transporter. However, the surviving G9KO mice gained body weight normally, but beyond age 37 weeks, only male G9KO mice weighed 17% less than controls.

**Hyperuricemia, Hyperuricosuria, and Polyuria in G9KO Mice.** Western blot analysis of whole kidney lysates from control and G9KO

Author contributions: F.P., O.B., and B.T. designed research; F.P., O.B., A.L., S.R., D.F., A.D.C., and S.M. performed research; F.P., O.B., A.L., S.R., and B.T. analyzed data; and F.P., O.B., and B.T. wrote the paper.

The authors declare no conflict of interest.

This article is a PNAS Direct Submission.

[1]F.P. and O.B. contributed equally to this work.

[2]To whom correspondence should be addressed. E-mail: bernard.thorens@unil.ch.

This article contains supporting information online at www.pnas.org/cgi/content/full/0904411106/DCSupplemental.

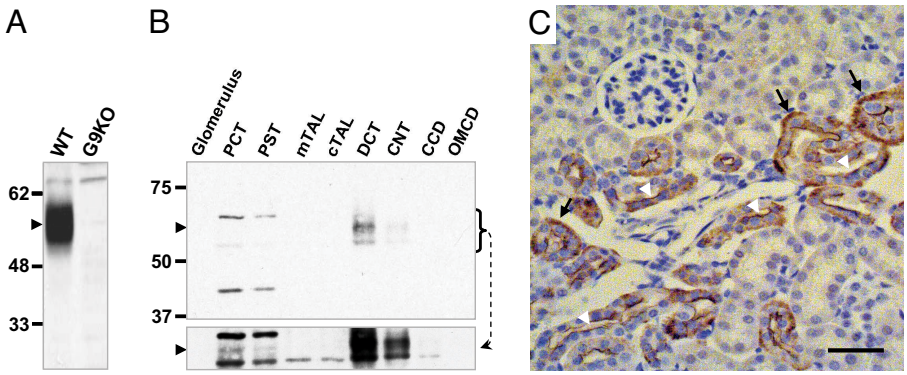


**Fig. 1.** Glut9 is expressed in the apical and basolateral membrane of distal convoluted tubules. (*A*) Western blot analysis of Glut9 expression (arrowhead) in whole kidney lysates from wild type (WT) and G9KO mice. The C-terminal directed antibody recognizes both the Glut9a and b isoforms. (*B*) Western blot analysis of Glut9 expression (arrowhead) in the indicated nephron segments: PCT, proximal convoluted tubule; PST: proximal straight tubule; mTAL: medullary thick ascending loop of Henle; cTAL: cortical thick ascending loop of Henle; DCT: distal convoluted tubule; CNT: connecting tubule; CCD: cortical collecting duct; OMCD: outer medulla collecting duct. A longer exposure time (lower panel) reveals a marginal expression of Glut9 in the PCT and PST. (*C*) Immunohistochemical detection of Glut9. Immunoreactivity is evident in the basolateral (black arrows) and apical (white arrowheads) membranes of cells from the distal tubule. (Scale bar, 50 $\mu$m.)

mouse kidneys revealed that Glut9 migrated as a single species of ≈55 kDa (Fig. 1*A*). Western blot analysis of microdissected nephron segments showed Glut9 expression mostly in the distal convoluted tubule (DCT) and in the connecting tubule (CNT), with a very faint band also observed in the proximal convoluted tubule (PCT) after longer exposure of the blot (Fig. 1*B*). Immunohistochemical analysis revealed that Glut9 is present in both the basolateral and apical membranes of the distal nephron (Fig. 1*C*); no detection in the PCT could be observed, probably due to the very low level of expression in this nephron segment. Thus, Glut9 may be involved in both steps of transepithelial urate transport, mostly in the distal tubule. We also confirmed that Glut9 is expressed at the plasma membrane of all hepatocytes (20) (Fig. S2).

We next measured plasma and urine urate levels in male and female mice. Plasma urate levels were higher in knockout than in heterozygous or wild-type mice (Fig. 2*A*). The urine urate concentrations were markedly (5- to 10-fold) higher in knockout mice as compared to heterozygous and wild type mice (Fig. 2*B*). Fractional excretion of urate was 4–5% in control mice indicating that 95% of filtered urate was reabsorbed (Fig. 2*C*). In male G9KO mice, fractional excretion was ≈100%, indicating severely suppressed urate reabsorption. Fractional excretion of urate in female G9KO mice was ≈150%, indicating suppressed urate reabsorption together with increased tubular excretion. In *Glut9*$^{+/-}$ mice, plasma and urine urate concentrations, and fractional excretion of urate were normal (Fig. 2 *A*–*C*).

Mice from all genotypes were then analyzed in metabolic cages. Daily food intake was similar in all three mouse groups and body weight did not vary significantly during the measurement period. Fecal weight and appearance were not significantly different among the three groups. Twenty-four–hour urate excretion was similar in Glut9$^{+/-}$ and WT mice. In G9KO mice, however, 24-h urate excretion was increased 20- to 30-fold (Fig. 2*D*), in association with increased water intake (Fig. 2*F*) and an approximately 5-fold higher 24-h urine volume (Fig. 2*E*) with a markedly lower urine osmolality (Fig. 2*G*). Upon water deprivation, urine osmolality dramatically increased in the control

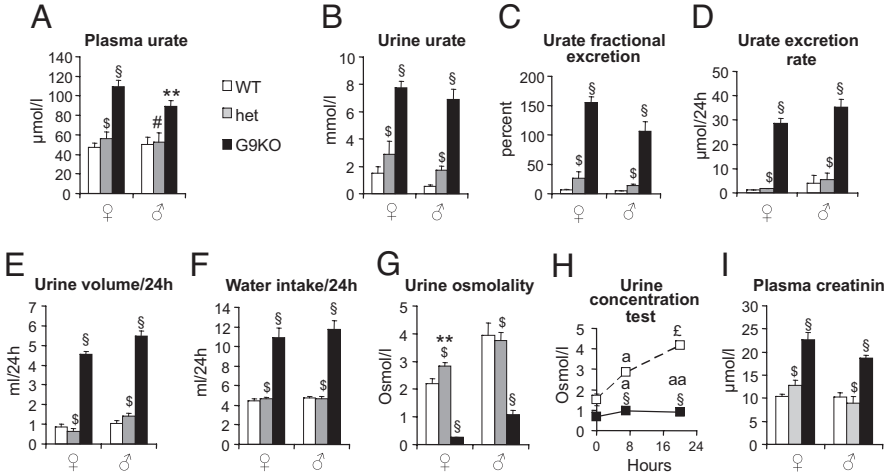


**Fig. 2.** G9KO mice are hyperuricosuric, polyuric, and polydipsic. (*A*) Urate concentration in plasma, (*B*) urate concentration in urine, (*C*) fractional excretion rate of urate; 10-week-old male and female mice. $n$ = 15 WT, 9 HET, 16 G9KO females, and 9 WT, 8 HET, 10 G9KO males. (*D*–*G*) Twenty-four hour analysis of electrolytes and water balance in 6-week-old male and female mice placed in metabolic cages. (*D*) urate excretion rate, (*E*) urine volume, (*F*) water intake, (*G*) urine osmolality. (*H*) Urine concentration test in female mice; (*I*) Plasma creatinine levels in 10-week-old male and female mice. $n$ = 15 WT, 9 HET, 16 G9KO females, and 9 WT, 8 HET, 10 G9KO males. Data are expressed as means ± SE. *, $P < 0.05$; **, $P < 0.01$; §, $P < 0.001$ vs. WT controls; #, $P < 0.05$; ##, $P < 0.01$; $, $P < 0.001$ vs. G9KO. For urine concentration test: a, $P < 0.05$; aa, $P < 0.01$; £, $P < 0.001$ vs. baseline.

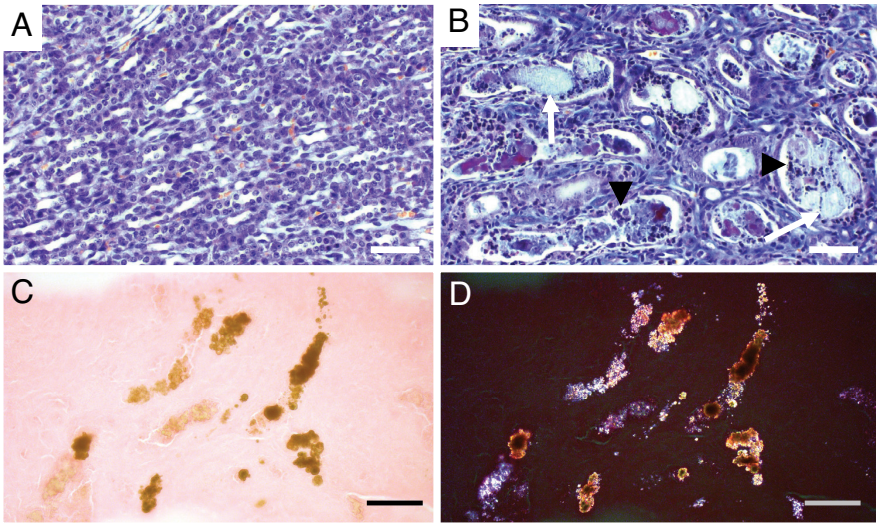


**Fig. 3.** Intratubular lithiasis in the kidney of 2-week-old G9KO mice. (*A* and *B*) FAOG staining showing normal medullary tubules in wild type controls (*A*) but precipitates (arrows) surrounded by inflammatory cells (arrowheads) in the intratubular space of G9KO medullary tubules (*B*). (*C* and *D*) Ethanol-fixed, eosin-stained G9KO kidney sections under direct (*C*) and polarized (*D*) light demonstrating anisotropic urate crystals in medullary renal tubules. (Scale bar, 100 $\mu$m.)

mice but not in the G9KO mice (Fig. 2*H*), indicating a urinary concentrating defect. Acidic urinary pH predisposes to urate precipitation and stone formation. Spot urine pH was below the $pK_a$ of urate (≈5.8) in 10-day-old wild-type pups (5.37 ± 0.06, $n = 12$) and was 5.84 ± 0.15 ($n = 30$) in 2-week-old pups. Spot urine pH was significantly lower in 6-week-old G9KO than in wild type mice (5.82 ± 038, $n = 11$ vs. 7.19 ± 0.78, $n = 8$, $P < 0.001$).

Plasma creatinine levels were higher in G9KO than in WT mice, suggesting impaired glomerular filtration rate (Fig. 2*I*). Plasma electrolytes showed minimal, if any, differences between G9KO and WT mice. However, G9KO mice exhibited mildly increased fractional excretion of $Na^+$, $K^+$, $Mg^{2+}$, and phosphate, without change in fractional excretion of $Ca^{2+}$ and no proteinuria or glucosuria was detected in G9KO mice (Table S1).

Thus, *Glut9* gene inactivation in mice led to a moderate hyperuricemia and a massively elevated uricosuria associated with renal insufficiency and a urinary concentrating defect.

**Glut9KO Mice Develop Urate Nephropathy.** Morphological analysis in newborn Glut9KO mice revealed normal kidney organogenesis, but discrete signs of tubule dilatation without fibrosis or inflammation. At 2 weeks of age, papillary tubular lumina were obstructed by granular material (Fig. 3*B*) that was birefringent under polarized light, consistent with urate crystals (Fig. 3 *C* and *D*). The intratubular deposits were surrounded by aggregates of mononuclear inflammatory cells and by desquamated tubular epithelial cells (Fig. 3*B*). Marked hydronephrosis was present in 6-week-old G9KO mice, as compared to WT controls (Fig. 4 *A–D*). About 30% of the superficial cortex exhibited areas of tubular atrophy with interstitial fibrosis (Fig. 4 *C–F*). Chronic interstitial inflammation was present in the fibrotic areas, as demonstrated by immunohistochemical detection of macrophages in the G9KO kidney cortical region (Fig. 4 *G* and *H*). At 16 weeks of age, interstitial fibrosis with tubular atrophy involved about 50% of the superficial renal cortex of G9KO mice. Severe chronic interstitial inflammation in fibrotic areas included lymphocytes organized in follicles with macrophages and fibroblasts in the cortico-medullar junction, sometimes extending to the calices. The granular precipitates in the lumens of atrophic tubules were surrounded by a severe chronic inflammation and interstitial fibrosis. Bladder stones were not found in G9KO mice, further glomerular sclerosis and vessel lesions were never observed. Kidneys of *Glut9*$^{+/-}$ mice appeared normal.

Thus, G9KO mice showed progressive and severe chronic tubulo-interstitial nephritis with cortical atrophy and hydronephrosis, likely secondary to tubular precipitation of urate. Microcystic tubules and hydronephrosis were consistent with obstructive nephropathy secondary to intratubular obstruction. This pathological description resembles that of human urate nephropathy.

Liver histology and plasma levels of ALT and AST were normal in G9KO mice (Fig. S3).

**Generation of Liver-Specific Glut9 Knockout Mice.** The increased total daily urate excretion in the G9KO mice suggested that normal degradation of urate by the hepatic enzyme uricase was impaired as a consequence of suppressed liver urate uptake in the absence of Glut9. We thus generated *Alb-CreERT2*;*Glut9*$^{lox/lox}$ mice, inactivated Glut9 in hepatoctytes by tamoxifen injection, and assessed urate homeostasis in these mice. Western blot analysis showed complete suppression of Glut9 protein expression in the liver of tamoxifen-treated *Alb-CreERT2*;*Glut9*$^{lox/lox}$ (LG9KO) mice and partial reduction in the liver of *Alb-CreERT2*; *Glut9*$^{lox/+}$ mice; Glut9 expression in the kidney of the tamoxifen-treated mice was not modified (Fig. S4).

**Liver-Specific Glut9KO Mice Are Hyperuricemic, Hyperuricosuric, and Polyuric.** Two weeks after tamoxifen treatment, plasma urate levels were markedly elevated (Fig. 5*A*) and uricosuria was increased 20-fold in both female and male LG9KO mice (Fig. 5*B*). Fractional excretion of urate was ≈25% in both female and male mutant mice, suggesting saturation of the renal urate reabsorption capacity in face of the massive hyperuricosuria and/or impaired urate reabsorption; however, this fractional excretion was much lower than in G9KO mice (Fig. 5*C* and see Fig. 2*C*). Daily urate excretion in LG9KO mice was elevated to ≈20 $\mu$mol/24 h (Fig. 5*D*), values comparable to those in G9KO mice (Fig. 2*D*). Urine volume was increased ≈2-fold in LG9KO mice (Fig. 5*E*) along with a tendency for higher water intake, as compared to controls (Fig. 5*F*). The urine osmolality was also

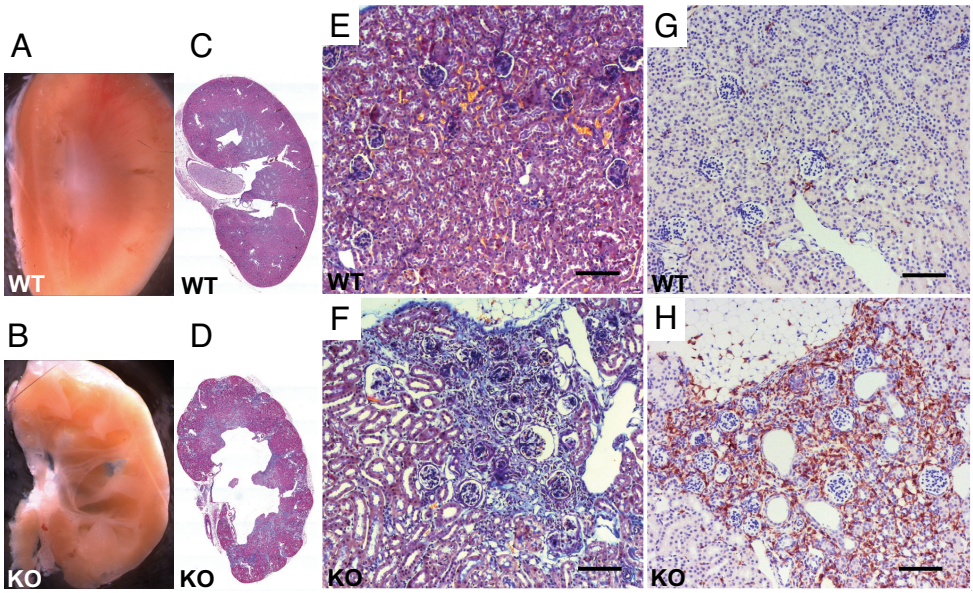


**Fig. 4.** Hydronephrosis and cortical fibrosis in the kidneys of adult G9KO mice. (*A*, *C*, *E*, and *G*): WT, (*B*, *D*, *F*, and *H*) G9KO. (*B*) Hydronephrosis of G9KO kidneys. (*C and D*) Hematoxylin and eosin staining revealed the lobular pattern of G9KO kidney due to inflammation and fibrosis. (*E and F*) Trichome staining of a cortical region in control (*E*) and G9KO (*F*) mouse kidneys. In mutant mice, there was fibrosis around glomeruli and tubular dilatation. (*G and H*) The cortical fibrotic region of G9KO mice contains a large number of macrophages as revealed by F4/80 antigen detection. (Scale bar, 50 $\mu$m.)

reduced in the LG9KO mice (Fig. *5G*); this was associated with a defect in urine concentration upon water deprivation (Fig. *5H*).

Plasma creatinine levels were normal in LG9KO mice (Fig. *5I*). Plasma electrolytes did not differ from values in control mice. Urinary fractional excretion of $Na^+$ and $Mg^{2+}$ were mildly elevated in LG9KO mice. (Table S2). Urinary pH was lower in the LG9KO mice compared to wild type littermates (5.71 ± 0.24, $n = 10$ vs. 6.06 ± 0.24, $n = 10$, $P < 0.02$).

Kidney histology was normal in the LG9KO mice, even 7 weeks after Glut9 deletion with no sign of tubular destruction or crystal deposition (Fig. S5).

## Discussion

This study identifies Glut9 as a major regulator of urate homeostasis. We show that the systemic and liver-specific *Glut9* knockout mice develop similar increases in uricosuria and daily urinary excretion of urate, consistent with a role for Glut9 to transport urate into hepatocytes, the major site for urate breakdown into allantoin. The greater degree of hyperuricemia in LG9KO than in G9KO mice can be explained by the lower fractional excretion of urate in the LG9KO mice. This is consistent with a major role for Glut9 in renal urate reabsorption, still present in LG9KO mice but absent in G9KO mice.

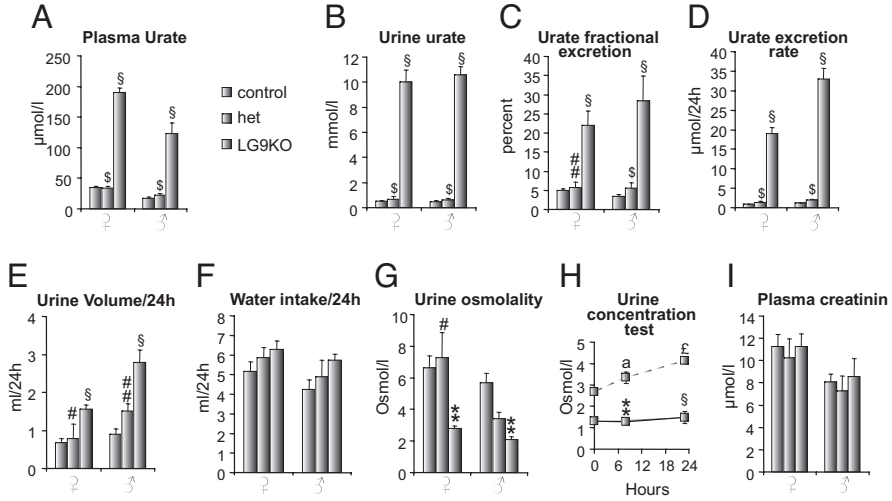


**Fig. 5.** LG9KO mice are hyperuricemic, hyperuricosuric, and polyuric. (*A*) Urate concentration in plasma, (*B*) urate concentration in urine, and (*C*) fractional excretion rate of urate; 24-week-old male and female mice, 2 weeks after tamoxifen-induced *Glut9* gene inactivation. $n = 12$ control, 4 HET, 8 LG9KO females, and 13 control, 6 HET, 5 LG9KO males. (*D–G*) Twenty-four hour analysis of electrolytes and water balance in mice placed in metabolic cages. (*D*) Urate excretion rate, (*E*) urine volume, (*F*) water intake, and (*G*) urine osmolality. (*H*) Urine concentrating test in female mice, and (*I*) plasma creatinine levels in 24-week-old male and female mice 2 weeks after tamoxifen induced *Glut9* gene inactivation. $n = 12$ control, 4 HET, 8 LG9KO females, and 13 control, 6 HET, 5 LG9KO males. Data are expressed as means ± SE. *, $P < 0.05$, **, $P < 0.01$; §, $P < 0.001$ vs. WT controls; #, $P < 0.05$; ##, $P < 0.01$; $, $P < 0.001$ vs. LG9KO. For urine concentration test: a, $P < 0.05$; aa, $P < 0.01$; £, $P < 0.001$ vs. baseline.

Despite similar hyperuricosuria and urate excretion, kidneys from LG9KO mice were morphologically normal, whereas the G9KO kidneys showed intratubular urate crystals deposition, inflammation, and tubulointerstitial fibrosis. Intriguing in this context is the defect in urine concentration capacity observed in both G9KO mice and LG9KO mice.

**Whole Body Glut9 Knockout Mice.** Urate homeostasis depends on the equilibrium between urate production and elimination. In the mouse, plasma urate levels are relatively low because urate is converted into allantoin by the hepatic enzyme uricase. Urate elimination depends on its glomerular filtration, complex tubular reabsorption, and secretion processes. A role for Glut9 in this process was recently proposed on the basis of genetic studies linking high uricemia with single nucleotide polymorphisms in the Glut9 gene and with observations that mutations in Glut9 were associated with lower uricemia in human patients (12, 18, 22). Functional studies have also shown that Glut9 is indeed a urate transporter (12, 18, 21). In contrast to the situation in humans (22), however, suppressing Glut9 function in mice leads to hyperuricemia, as a result of impaired uptake of urate by the liver and degradation by uricase.

Gene inactivation of other urate transport proteins URAT1, OAT1, and OAT3, which are located in the proximal convoluted tubule (23, 24), leads to only moderate dysregulation of urate homeostasis. In marked contrast, we show that *Glut9* gene inactivation leads to greatly elevated urate excretion and suppressed renal reabsorption with a fractional excretion of urate of 100% in G9KO mice. We show in microdissected mouse nephrons that Glut9 is mostly expressed in the distal convoluted tubule, although we cannot exclude a low level of expression in the PCT. In the distal tubule, Glut9 is present in both the basolateral and apical poles, suggesting that it can support both steps of urate transepithelial transport.

Interestingly, G9KO mice developed obstructive intratubular urate lithiasis at 2 weeks of age, a likely cause of the hydronephrosis and of the inflammatory reaction. Uric acid crystals are indeed known to induce inflammation secondary to activation of the inflammasome and the production of Il-1ß (5). At 6 weeks of age and later, the inflammatory reaction and fibrosis had spread over a large fraction of the cortex leading to reduction in tubular area.

The kidney of the G9KO mice showed impaired glomerular filtration, as suggested by elevated plasma creatinine concentrations. Furthermore, the urinary concentrating capacity was suppressed, as assessed by the response to water withdrawal. Although possibly secondary to the destruction of tubules in the medulla and papilla, the impaired concentrating capacity might arise from as yet unidentified mechanisms, since the concentrating defect is present also in LG9KO mice, which show no morphological alteration in the kidney.

**Liver-Specific Glut9 Knockout Mice.** As the liver is a major site of Glut9 expression, we assessed the physiological impact of selective *Glut9* gene inactivation in adult mouse hepatocytes. This induced hyperuricosuria and a 24-h urate excretion that was elevated to the same degree as in G9KO mice. These observations indicate that in the absence of liver Glut9, urate cannot be converted to allantoin, and most if not all of the body's urate load must be excreted in the urine. In contrast to the G9KO mice, the higher plasma urate levels found in these mice probably result from the intact urate reabsorption activity of kidney Glut9. Indeed, the fractional excretion rate in the LG9KO mice indicated that a significant amount of the filtrated urate was reabsorbed.

Strikingly, LG9KO mice had normal kidney morphology with no sign of crystal deposition. This is in contrast to the alterations seen in G9KO mice caused by urate crystals formed early after birth. Formation of urate crystals, at this early age, may be explained by several parameters. First, urine has a more acidic pH in newborn than in adult mice (see *Results*); second, there is a transient increase (3- to 4-fold) in uricosuria during the first 2 weeks of life in the mouse (25); third, suckling newborn mice may not compensate for polyuria-induced dehydration by increasing milk intake (26), hence limiting the possibility to dilute urine; fourth, newborn mice are highly susceptible to hypothermia (27) favoring crystal formation. The early formation of urate crystals and similar progressive kidney morphological alterations have also been observed in hyperuricemic, hyperuricosuric uricase knockout mice, despite native renal Glut9 expression (28). Once urate crystallization appears in the G9KO mice, it is associated with and likely exacerbated by influx and accumulation of inflammatory cells leading to tubular damage. These initial lesions are then perpetuated by the permanent hyperuricosuria.

The plasma urate levels obtained in the LG9KO mice approximate those observed in human plasma. Elevated urate levels are thought to protect against oxidative stress but also, at very high levels, to increase the risk of renal and cardiovascular diseases and gout. The LG9KO mice may thus serve in future studies to evaluate the role of elevated plasma urate levels in the development of the metabolic syndrome triggered by metabolic or inflammatory stresses.

Together, these studies define Glut9 as a major regulator of uric acid homeostasis. In kidney, Glut9 sustains urate reabsorption independently of the other known urate transporters URAT1, OAT1, and OAT3. Early hyperuricemia in G9KO mice induces a renal condition similar to acute urate nephropathy in humans. Study of G9KO mice may thus help delineate the pathogenic events causing this disease. Study of LG9KO mice has indicated the critical role of the liver in urate catabolism and the role of Glut9 in this process. These mice will be helpful in delineating the effect of chronically elevated urate plasma levels in the development of the metabolic syndrome.

## Materials and Methods

**Generation of Glut9 Knockout Mice.** Details of the preparation of whole body and liver-specific Glut9 knockout mice can be found in the *SI Text*. All animal studies were approved by the Service Vétérinaire du Canton de Vaud, Switzerland.

**Blood and Urine Chemistry.** Urine and plasma from retroorbital bleeds were collected at 10–12 AM. Plasma and urine chemistry was analyzed using the Roche/Hitachi 902 robot system (Roche), except for sodium and potassium, which were analyzed using a flame photometer (IL-943, Instrumentation Laboratory). Osmolality was assessed by a vapor pressure osmometer (Vapro 5520, Wescor Inc.). Fractional excretion rate of urate was calculated from urate and creatinine measurements.

**Metabolic Cages.** To measure water intake, urine volumes, and renal excretion of $Na^+$, $K^+$, $Ca^{2+}$, $Mg^{2+}$, phosphate, and glucose, mice were placed into individual metabolic cages. Food intake as well as feces weight were also measured. Mice were allowed to acclimate to the cages for 2 days before one or two cycles of 24-h measurements. Excretion rates were calculated as the total amount of each ion present in the urine volume collected over 24 h.

**Statistical Analyses.** Statistical analyses were performed using the Graphpad Prism 4.0 software (Graphpad Software Inc.). Comparisons between groups were performed using one-way ANOVA test followed by Bonferoni post hoc test. Paired or unpaired *t* test analysis was used for urine concentration and pH data.

**ACKNOWLEDGMENTS.** The authors thank Armelle Bauduret for mouse genotyping, Marianne Carrard for blood and urine analyses, Catherine Roger and Dr. Snezana Andrejevic Blunt for histological analyses, and David Tarussio for expert technical help. We thank Dr. Kaethi Geering and Dr. Seth Alper for critical reading of the manuscript. This work was supported by grants to B.T. from the Swiss National Science Foundation No. 31003A-113525, the European Union FP6 program on Hepatic and Adipose Tissue and Functions in the Metabolic Syndrome (EU-FP6 HEPADIP), and the FP7 program on European Drug Initiative on Channels and Transporters (EU-FP7 EDICT). O.B.'s work is supported by a Foundation Prof. Placide Nicod grant and by a bridge grant from the Faculté de Biologie et Médecine de l'Université de Lausanne.

1. Hayden MR, Tyagi SC (2004) Uric acid: A new look at an old risk marker for cardiovascular disease, metabolic syndrome, and type 2 diabetes mellitus: The urate redox shuttle. *Nutr Metab (Lond)* 1:10–25.
2. Feig DI, Kang DH, Johnson RJ (2008) Uric acid and cardiovascular risk. *N Engl J Med* 359:1811–1821.
3. Mene P, Punzo G (2008) Uric acid: Bystander or culprit in hypertension and progressive renal disease? *J Hypertens* 26:2085–2092.
4. Petrilli V, Dostert C, Muruve DA, Tschopp J (2007) The inflammasome: A danger sensing complex triggering innate immunity. *Curr Opin Immunol* 19:615–622.
5. Martinon F, Petrilli V, Mayor A, Tardivel A, Tschopp J (2006) Gout-associated uric acid crystals activate the NALP3 inflammasome. *Nature* 440:237–241.
6. Kang DH, Nakagawa T (2005) Uric acid and chronic renal disease: Possible implication of hyperuricemia on progression of renal disease. *Semin Nephrol* 25:43–49.
7. Rampello E, Fricia T, Malaguarnera M (2006) The management of tumor lysis syndrome. *Nat Clin Pract Oncol* 3:438–447.
8. Hediger MA, Johnson RJ, Miyazaki H, Endou H (2005) Molecular physiology of urate transport. *Physiology (Bethesda)* 20:125–133.
9. Enomoto A, et al. (2002) Molecular identification of a renal urate anion exchanger that regulates blood urate levels. *Nature* 417:447–452.
10. Eraly SA, et al. (2008) Multiple organic anion transporters contribute to net renal excretion of uric acid. *Physiol Genomics* 33:180–192.
11. Hagos Y, Stein D, Ugele B, Burckhardt G, Bahn A (2007) Human renal organic anion transporter 4 operates as an asymmetric urate transporter. *J Am Soc Nephrol* 18:430–439.
12. Anzai N, et al. (2008) Plasma urate level is directly regulated by a voltage-driven urate efflux transporter URATv1 (SLC2A9) in humans. *J Biol Chem* 283:26834–26838.
13. Sekine T, Watanabe N, Hosoyamada M, Kanai Y, Endou H (1997) Expression cloning and characterization of a novel multispecific organic anion transporter. *J Biol Chem* 272:18526–18529.
14. Bakhiya A, Bahn A, Burckhardt G, Wolff N (2003) Human organic anion transporter 3 (hOAT3) can operate as an exchanger and mediate secretory urate flux. *Cell Physiol Biochem* 13:249–256.
15. Li S, et al. (2007) The GLUT9 gene is associated with serum uric acid levels in Sardinia and Chianti cohorts. *PLoS Genet* 3:e194.
16. Dehghan A, et al. (2008) Association of three genetic loci with uric acid concentration and risk of gout: A genome-wide association study. *Lancet* 372:1953–1961.
17. Doring A, et al. (2008) SLC2A9 influences uric acid concentrations with pronounced sex-specific effects. *Nat Genet* 40:430–436.
18. Vitart V, et al. (2008) SLC2A9 is a newly identified urate transporter influencing serum urate concentration, urate excretion and gout. *Nat Genet* 40:437–442.
19. Augustin R, et al. (2004) Identification and characterization of human glucose transporter-like protein-9 (GLUT9): Alternative splicing alters trafficking. *J Biol Chem* 279:16229–16236.
20. Keembiyehetty C, et al. (2006) Mouse glucose transporter 9 splice variants are expressed in adult liver and kidney and are up-regulated in diabetes. *Mol Endocrinol* 20:686–697.
21. Caulfield MJ, et al. (2008) SLC2A9 is a high capacity urate transporter in humans. *PLoS Med* 5:e197.
22. Matsuo H, et al. (2008) Mutations in glucose transporter 9 gene SLC2A9 cause renal hypouricemia. *Am J Hum Genet* 83:744–751.
23. Hosoyamada M, Ichida K, Enomoto A, Hosoya T, Endou H (2004) Function and localization of urate transporter 1 in mouse kidney. *J Am Soc Nephrol* 15:261–268.
24. Sekine T, Miyazaki H, Endou H (2006) Molecular physiology of renal organic anion transporters. *Am J Physiol Renal Physiol* 290:F251–261.
25. Kelly SJ, et al. (2001) Diabetes insipidus in uricase-deficient mice: A model for evaluating therapy with poly(ethylene glycol)-modified uricase. *J Am Soc Nephrol* 12:1001–1009.
26. Blass EM, Teicher MH (1980) Suckling. *Science* 210:15–22.
27. Goodrich CA (1977) Measurement of body temperature in neonatal mice. *J Appl Physiol* 43:1102–1105.
28. Wu X, et al. (1994) Hyperuricemia and urate nephropathy in urate oxidase-deficient mice. *Proc Natl Acad Sci USA* 91:742–746.